Published in final edited form as:
Neuroscience. 2012 September 6; 219: 271–279. doi:10.1016/j.neuroscience.2012.05.064.

Transient mGlu5 receptor inhibition enhances the survival of granule cell precursors in the neonatal cerebellum

Cathryn Kubera, **Amanda L. Hernandez**, **Vibol Heng**, and **Angélique Bordey**
Departments of Neurosurgery, and Cellular and Molecular Physiology, Yale University School of Medicine, New Haven, CT 06520-8082

Abstract

The generation of the most abundant neurons of the cerebellum, the granule cells, relies on a balance between clonal expansion and apoptosis during the first 10 days after birth in the external germinal layer (EGL). The amino acid glutamate controls such critical phases of cell development in other systems through specific receptors such as metabotropic glutamate receptor 5 ($mGlu_5R$). However, the function of $mGlu_5Rs$ on the proliferation and survival of granule cell precursors (GCPs) remains elusive. We found $mGlu_5R$ mRNA transcripts in EGL using RT-PCR and observed $mGlu_5R$-mediated Ca^{2+} responses in GCPs in acute slices as early as postnatal day (P) 2–3. Using *in vivo* injections of the selective non-competitive $mGlu_5R$ antagonist 2-Methyl-6-(phenylethynyl)pyridine (MPEP) in P7–9 mice, we found a 20% increase in the number of proliferative GCPs labeled at P7 with the S-phase marker bromodeoxyuridine (BrdU), but no increase in cell proliferation examined 2 hours following a BrdU injection. Furthermore, similar treatments led to a significant 70% decrease in the number of apoptotic GCPs in the EGL as determined by TUNEL staining. In contrast, *in vivo* treatment with the $mGlu_5R$ agonist (*RS*)-2-Chloro-5-hydroxyphenylglycine (CHPG) resulted in a ~60% increase in the number of TUNEL-labeled GCPs compared to control. These findings identify a unique role for glutamate acting at $mGlu_5Rs$ as a functional switch regulating GCP survival in the EGL, thus controlling the total number of cerebellar granule cells produced.

Keywords

glutamate receptor; neurogenesis; neuronal precursors; metaboptic glutamate receptor; proliferation; apoptosis

INTRODUCTION

The development of the postnatal cerebellum, and specifically that of the cerebellar granule cells, can be subdivided into distinct stages. Granule cell precursors (GCPs) proliferate in the outer external germinal layer (EGL) up to two weeks postnatal. Between postnatal days 6 and 9 in rodents, a percentage of the proliferating GCPs undergo apoptosis (Tanaka and Marunouchi, 1998; Wood et al., 1993). Upon cell cycle exit, GCPs migrate tangentially in the inner EGL, then turn and migrate radially to the inner granular layer (IGL) where they

Address for correspondence: Angélique Bordey, Ph.D., Yale Univ. Sch. Med. 333 Cedar St, FMB 422, New Haven, CT 06520-8082, Phone: 203-737-2515, Fax: 203-737-2159, angelique.bordey@yale.edu.

synaptically integrate (Altman, 1969; Goldowitz and Hamre, 1998; Hatten and Heintz, 1995; Mullen et al., 1997). Signals regulating GCP proliferation and survival are critical for controlling the ultimate number of newborn GCPs that are necessary for proper circuit formation and function.

One of these signals is the amino acid and neurotransmitter glutamate. Glutamate acting at several specific receptors controls several stages of cell development (Nguyen et al., 2001; Platel et al., 2010). One family of these receptors, the metabotropic glutamate receptor (mGluR) family, have been implicated in cell proliferation and survival in various neurogenic regions throughout the brain (Brazel et al., 2005; Castiglione et al., 2008; Di Giorgi-Gerevini et al., 2005). Of the eight mGluRs, $mGlu_4R$ and $mGlu_5R$ may be expressed in the EGL (Copani et al., 1998; Corti et al., 2002; Di Giorgi Gerevini et al., 2004). Indeed, injection of a $mGlu_4R$ agonist *in vivo* has been shown to reduce GCP proliferation and promote differentiation in lobule V only (Canudas et al., 2004). Injections of $mGlu_5R$ antisense in the neonatal cerebellum have been shown to reduce granule cell density in the IGL, but the EGL was not examined (Catania et al., 2001). Studies done in culture have conflicting outcomes as to whether $mGlu_5R$ promotes cell survival or not (Battaglia et al., 2001; Bruno et al., 2000; Catania et al., 2001; Copani et al., 1998; D'Antoni et al., 2011; Di Giorgi-Gerevini et al., 2005). However, the role of $mGlu_5Rs$ has not been explored in the EGL.

$mGlu_5Rs$ are G-protein coupled receptors leading to Ca^{2+} increases through inositol trisphosphate. Activation of these receptors is thus expected to regulate the behavior of GCPs through Ca^{2+} increases. Indeed, Ca^{2+} activity is tightly correlated with progression through the cell cycle and cell migration including the tangential migration of GCPs in the inner EGL (Komuro and Rakic, 1996; Komuro and Rakic, 1998; Parkash and Asotra, 2010).

Interestingly, $mGlu_5R$ has been shown to be misregulated in a number of developmental disorders, including Fragile X Syndrome, autism, tuberous sclerosis, and Attention Deficit Hyperactivity disorder (Boer et al., 2008; Carlson, 2012; Dolen and Bear, 2008a; Elia et al., 2012). Although all of these developmental disorders are typically thought of as cortical cerebral in nature, they all have a cerebellar pathology as well (Casanova, 2007; Fatemi et al., 2008; Huber, 2006; Koekkoek et al., 2005; Marti-Bonmati et al., 2000). In addition to its role in motor control, the cerebellum is now well-known to have cognitive and affective functions (Baillieux et al., 2008). Considering that selective $mGlu_5R$ antagonists are in clinical trials for treatment of Fragile X syndrome and autism, it is important to know the effects of these drugs on the development of all brain systems, including the cerebellum.

In this study, we focused on $mGlu_5Rs$ and sought to determine its role in GCP proliferation and survival in the EGL of the postnatal murine cerebellum. We found that activation of $mGlu_5Rs$ led to Ca^{2+} increases in GCPs of the EGL. *In vivo* injection of the non-competitive $mGlu_5R$ antagonist 2-Methyl-6-(phenylethynyl)pyridine hydrochloride (MPEP) resulted in a significant decrease in the number of apoptotic GCPs in the EGL. In contrast, *in vivo* injection of the $mGlu_5R$ agonist (*RS*)-2-Chloro-5-hydroxyphenylglycine (CHPG) had the opposite effect. These findings identify a unique role for $mGlu_5Rs$ in the number of apoptotic cells during postnatal cerebellar development and suggest that $mGlu_5Rs$ may be a deciding factor in determining the total number of cerebellar granule cells.

EXPERIMENTAL PROCEDURES

Animals

CD-1 mice of either gender were obtained from Charles River Laboratories (Boston, MA). All experiments were performed in accordance with Yale Animal Care and Use Committee guidelines.

RT-PCR for $mGlu_5R$ transcripts

1 or 10 cells were extracted from the EGL of P7–P12 acute horizontal cerebellar slices using a pulled glass patch pipet containing a solution of water, 23 mM DTT, and 4 units μl^{-1} RNase inhibitor (Applied Biosystems, Foster City, CA). The pipet tip was then broken into a pcr tube containing reagents for reverse transcription (High Capacity cDNA Reverse Transcription Kit, Applied Biosystems, Foster City, CA), and the reaction was run in a MyCycler Thermal Cycler (BioRad, Hercules, CA) according to kit instructions. Once the mRNA was converted to cDNA, 36 cycles of PCR amplification were performed using Platinum *Taq* polymerase reagents (Invitrogen, Carlsbad, CA) and primers for $mGlu_5R$: forward 5′-GTCCTTCTGTTGATCCTGTC-3′; reverse 5′-ATGCAGCATGGCCTCCACTC-3′ (product size: 216 bp). A second round of PCR (36 cycles) was performed using fresh master mix and 3μl of sample from the first reaction. End point PCR product was resolved on a 2% agarose gel in TAE buffer.

Calcium imaging

Acute sagittal or horizontal cerebellum brain slices were prepared from P2–P4 or P7–P12 mouse pups. Mice were anesthetized with pentobarbital (50 $mgkg^{-1}$) via intraperitoneal (IP) injection, decapitated, and the brain was rapidly removed into ice cold oxygenated artificial cerebrospinal fluid (aCSF) containing (in mM): NaCl 125; KCl 2.5; $CaCl_2$ 1.8; $MgCl_2$ 1; $NaHCO_3$ 25; glucose 10 as previously reported (Dave and Bordey, 2009). 300 μm sagittal or horizontal sections were cut using a Leica VT 1000S vibrating microtome and placed in a recovery chamber containing oxygenated aCSF at room temperature for 30–60 minutes prior to loading. To load Ca^{2+} indicator dyes, slices were incubated with 5 μM Fluo-4 AM + 5 μM Oregon Green BAPTA AM (OGB) + 0.02% F-127 pluronic acid (Invitrogen, Carlsbad, CA) in aCSF for 30–45 minutes at 37° C. Loaded slices were placed in a flow-through chamber and continuously perfused with oxygenated aCSF for 30 minutes prior to imaging to allow for de-esterification. Two to five minute Ca^{2+} imaging movies were taken in a single plane with an acquisition rate of 1.12 frames s^{-1} using an Olympus Fluoview 300 confocal microscope equipped with a 60x water immersion objective lens. 50–100 μM (*S*)-3,5-dihydroxyphenylglycine (DHPG) or 500–1000 μM (*RS*)-2-Chloro-5-hydroxyphenylglycine (CHPG) (both Tocris Bioscience, Ellisville, MO) was presented to cells of the EGL using pressure application (3 psi) for 30–120 s. Antagonists were bath applied through the perfusion system. Following movie acquisition, Ca^{2+} imaging data were analyzed using CalSignal software developed by JC Platel (Platel et al., 2007), Microsoft Excel 2007 and Microcal Origin 6.0.

Drug Injections

MPEP hydrochloride (Tocris Bioscience, Ellisville, MO) was given twice daily 8–12 hours apart intraperitoneally (IP) at 15 mg kg^{-1} on postnatal days (P)7-P9. MPEP was dissolved at 1mg ml^{-1} in phosphate buffered saline (PBS). Mice in the control group were given an equal volume of PBS alone. For BrdU-labeling experiments, all mice received one IP injection of BrdU (50 $\mu g\ g^{-1}$) along with either the first or last drug injection. CHPG was given intracerebroventricularly (icv) once per day for two days beginning at P2. Pups were anesthetized on ice and 1–5 μl of 25 mM CHPG in sterile PBS with 0.02% Fast Green dye

was injected into the lateral ventricle with manual pressure using a pulled glass pipet beveled to a <50 μm diameter. Mice in the control group were given an equal volume of PBS plus 0.02% Fast Green.

Immunostaining

Sample preparation and immunostaining were performed as previously described (Platel et al., 2009). Briefly, P9 mice were anesthetized with pentobarbital (50 mg kg^{-1} via IP injection) and decapitated. The brains were rapidly removed and drop-fixed in 4% paraformaldehyde overnight at 4°C. For BrdU staining, free-floating sagittal brain sections (100 μm) were treated with 2N HCl for 1 hour at room temperature. Sections were washed with PBS and then blocked in PBS blocking solution (PBS plus 0.1% Tween-20, 0.1% Triton X-100, 2% bovine serum albumin) for an additional hour. Primary antibodies (1:100 anti-BrdU BU1/75, Accurate Chemical & Scientific Corporation, Westbury, NY) were applied overnight at 4°C. Sections were washed with multiple changes of PBS + 0.05% Tween-20 (PBS-T) and then incubated in secondary antibodies (1:1000 goat anti-rat Alexa Fluor 555, 1:10000 DAPI; Invitrogen, Carlsbad, CA) for one hour at room temperature. Following several washes sections were mounted on glass slides with Prolong Gold Antifade (Invitrogen, Carlsbad, CA).

Terminal deoxynucleotidyl transferase dUTP nick end labeling (TUNEL) was performed using the ApopTag Fluorescein In Situ Apoptosis Detection Kit (Millipore, Billerica, MA) on 50 μm-thick cryostat sections from P3 or P9 mice mounted on gelatin-coated glass slides. Slides were then incubated with 1:10000 DAPI for 10 min and washed briefly. Coverslips were mounted with Prolong Gold Antifade. Slides were imaged on an Olympus FluoView 1000 confocal microscope.

Analysis

For quantification of BrdU positive cells in the EGL, 40x images were taken in the region between folia V and VI in mid-sagittal cerebellum sections. Researchers were blinded to files and manually counted DAPI-positive and BrdU-positive cells in the EGL using Image J software (Rasband, W.S, US National Institutes of Health, Bethesda, MD). The percent of BrdU-positive cells was determined by dividing the number of BrdU-positive EGL cells by the number of DAPI-positive EGL cells per image and normalizing to control. For quantification of TUNEL-positive cells, Z-projections of image stacks spanning 16 μm were made using Image J. Overlapping images from along the primary fissure between folia V and VI in P9 mice, or from the entire cerebellum in P3 mice, were fit together using the stitching plugin (Preibisch et al., 2009). Researchers were blinded to files and the number of TUNEL-positive cells in the EGL was manually counted. The area of the EGL was quantified by outlining a region of interest around the EGL, defined by DAPI labeling, and using the Measure function in Image J. Calculations to determine average TUNEL-positive cells per mm^3 were done in Microsoft Excel.

Quantitative Real Time PCR Apoptosis Array

cDNAs were prepared from 10 cell aspirates from the EGL of P9 CD1 mice treated with either PBS or MPEP using the RT^2 Nano PreAMP cDNA Synthesis Kit (SA Biosciences, Frederick, MD). cDNAs were pre-amplified for 12 cycles of PCR with SA Biosciences apoptosis array primer mix and 2x RT^2 PreAMP PCR Master Mix. Pre-amplified templates were then combined with nuclease-free double distilled water and 2x RT^2 qPCR Sybr Green Master Mix and 10 μl per well was loaded onto a 384-well plate SA Biosciences Mouse Apoptosis PCR Array (catalog # PAMM-012). PCR was run for 40 cycles of 95°C for 15 s, 60°C for 60 s on an Applied Biosystems 7900HT Fast Real-Time PCR System. C_t values

were put into Excel-based PCR Array Data Analysis Software from SA Biosciences to calculate relative gene expression, fold regulation, and p-values.

Statistics

Values are expressed as mean ± standard error of the mean (sem) unless otherwise stated. Significance was set at $p < 0.05$.

RESULTS

Functional presence of $mGlu_5$Rs in the EGL

We used RT-PCR to test for $mGlu_5$R expression in cellular aspirates from the EGL of P7–P12 acute horizontal cerebellar slices. Electrophoresis of $mGlu_5$R PCR product revealed a band at the expected size of 216 bp in a 10 cell-sample, suggesting the presence of $mGlu_5$R mRNA in the EGL (Fig. 1A).

To examine whether $mGlu_5$R, a G_q-coupled receptor, was functional in GCPs, we performed Ca^{2+} imaging in acute slice preparations from animals at two different postnatal timepoints. P2–P3 or P7–P12 horizontal cerebellar slices were bath loaded with the Ca^{2+} indicator dyes Fluo-4 AM and Oregon Green BAPTA AM (5 μM each). A 30–120 s-pressure application of the $mGlu_5$R agonist DHPG (50–100 μM) increased Ca^{2+} levels in ~25% of GCPs in the EGL of P2–P3 slices (n=3 slices, 12–24 cells per slice) and ~34% of GCPs in the EGL of P7–P12 slices (n=6 slices, 5–20 cells per slice, Fig. 1B and C at P7–P12). DHPG-induced Ca^{2+} elevations were inhibited by bath application of MPEP or MTEP (25–60 μM), which are selective $mGlu_5$R antagonists (n=3 slices at P2–P3, n=6 slices at P7–P12, Fig. 1D and E). Pseudo-colored Ca^{2+} images and Ca^{2+} activity traces are shown in Figure 1 (B and D) and (C and E), respectively. The mean Ca^{2+} traces of all DHPG responding cells at P7–P12 are shown in Figure 1F. GCPs in the EGL also responded to the $mGlu_5$R-selective agonist CHPG (500 μM-1 mM) with intracellular Ca^{2+} increases (n=4 slices at P2–P3 and 3 slices at P7–P9, traces not shown). Quantification of the area under the Ca^{2+} responses during the first 30 s of agonist applications revealed that DHPG and CHPG induced Ca^{2+} responses of similar area at both ages (Fig. 1G and H). These data show that $mGlu_5$R activation leads to Ca^{2+} increases in GCPs in the EGL, suggesting the presence of functional $mGlu_5$Rs.

$mGlu_5$R inhibition *in vivo* increases BrdU labeling and cell survival in the EGL

Cell proliferation in the EGL following *in vivo* inhibition of $mGlu_5$Rs was studied using BrdU labeling at the time of the first MPEP injection (Fig. 2A). BrdU labeling was analyzed between folia V and VI (Fig. 2B). Subsequent to MPEP administration (2 injections per day, for 3 days), the number of BrdU-positive cells in the EGL was increased by ~20% compared to PBS-injected controls (Fig. 2C–I). However, there was no significant difference in the number of BrdU-labeled cells in the EGL when BrdU was administered along with the final PBS or MPEP injection on P9 (Fig. 2C), suggesting no effect of $mGlu_5$R on GCP proliferation. To examine whether MPEP prevented GCP migration out of the EGL, GCP radial migration in acute cerebellar slices was monitored for two hours (one hour in control aCSF followed by one hour in control aCSF or 60 μM MPEP). We found no difference in GCP migration speed in MPEP compared to control conditions (data not shown).

Increased cell survival following *in vivo* MPEP treatment could also account for the increase in BrdU-positive cells in the EGL. TUNEL staining was performed on sagittal cerebellar sections from P9 mice treated with either MPEP or PBS (same treatment as above, Fig. 3A–C). In the EGL along the primary fissure between folia V and VI TUNEL staining labeled $5.5 \pm 0.9 \times 10^4$ cells/mm^3 in control compared to $1.5 \pm 0.4 \times 10^4$ cells/mm^3 with MPEP

treatment ($p < 0.05$, paired Student's t test, 9 sections, 3 animals each, Fig. 3C). This equates to a 73% reduction in TUNEL staining following $mGlu_5R$ inhibition (Fig. 3C). In addition, we tested the effect of icv injections of the $mGlu_5R$ agonist CHPG in P2–P3 pups (1 injection/day for 2 days, 25–100 nmol/pup). CHPG injections resulted in an increase in the number of TUNEL-positive cells in the EGL ($3.8 \pm 0.7 \times 10^4$ in control compared to $6.1 \pm 0.7 \times 10^4$ cells/mm^3 with CHPG, $p < 0.05$, paired t test, 9 sections, 3 animals each, Fig. 3D and E). Thus, tonic $mGlu_5Rs$ activation regulates the number of apoptotic GCPs in the EGL.

Gene regulation supports a role for $mGlu_5R$ in GCP apoptosis

To examine whether MPEP treatment altered the expression of apoptotic genes in the EGL, qRT-PCR for apoptosis related genes was run on cells isolated from the EGL in MPEP or PBS treated animals (Fig. 4). Of 84 genes in an array, we reliably detected signal for 21 apoptosis-related genes, plus 4 house-keeping genes (Table 1). Anti-apoptosis genes were found to be up-regulated while pro-apoptotic genes were down-regulated or did not change with MPEP treatment (Fig. 4A and B). Of the anti-apoptotic genes examined, a moderate increase in Apoptosis inhibitor 5 (Api5) was detected following MPEP administration. Of the pro-apoptotic genes examined, BCL2-related ovarian killer protein (Bok), Caspase 14 (Casp14), CASP2 and RIPK1 domain containing adaptor with death domain (Cradd), CD40 antigen (Cd40), and Transformation related protein 53 inducible nuclear protein 1 (Trp53inp1) all had greater than 3-fold down-regulation in MPEP treatment conditions. The changes in Bok and Casp14 were found to be significant using a paired one-tailed Student's t-test ($p = 0.024$ and $p = 0.049$ for Bok and Casp14, respectively).

DISCUSSION

We report here the novel finding that inhibition of $mGlu_5R$ *in vivo* promotes the survival of GCPs in the EGL of the neonatal cerebellum while $mGlu_5R$ activation has an opposite effect. These findings suggest that tonic $mGlu_5R$ activation controls the number of GCPs prior to their migration and synaptic integration in the granule cell layer.

$mGlu_5R$ expression was found in the EGL using RT-PCR and Ca^{2+} imaging suggesting that these receptors are functional in the EGL. We then assessed the role of $mGlu_5Rs$ in GCP proliferation, migration, and survival. By pulse labeling dividing cells with BrdU prior to MPEP treatment, we found an increase in the number of BrdU-labeled GCPs in the EGL. However, no change in the rate of proliferation was found when GCPs were labeled with BrdU following MPEP treatment. In addition, we found no effect of MPEP on the speed of GCP radial migration of GCPs, which is consistent with the lack of effect on the tangential migration of neuroblasts in the postnatal subventricular zone and cultured oligodendroglial progenitor cells (Luyt et al., 2007; Platel et al., 2008).

Regarding proliferation, several studies have demonstrated a role for $mGlu_5Rs$ on the proliferation of neural progenitor cells, neuroblasts, and astrocytes (Di Giorgi-Gerevini et al., 2005; Gandhi et al., 2008; Kanumilli and Roberts, 2006; Melchiorri et al., 2007; Zhao et al., 2011). However, in these studies activation and not inhibition of $mGlu_5Rs$ increased the number of proliferative cells. In our study, it is likely that the increased number of BrdU-positive cells results from the increase in cell survival. Indeed we found that $mGlu_5R$ inhibition at the peak of GCP apoptosis in the EGL (Tanaka and Marunouchi, 1998; Wood et al., 1993) resulted in a 70% decrease in the number of TUNEL-positive cells. This finding was further supported by running a qRT-PCR apoptosis array on aspirates from the EGL of PBS- or MPEP-treated animals. Consistent with our TUNEL data, we found down-regulation of several pro-apoptotic genes in the MPEP-treated samples. Treating with a $mGlu_5R$ agonist (CHPG) *in vivo* results in a 60% increase in the number of apoptotic cells in the EGL. Our results indicate that $mGlu_5R$ inhibition decreased the number of apoptotic

cells, which contrasts with previous *in vitro* and one *in vivo* study (Catania et al., 2001; Copani et al., 1998).

In vivo knock-down of $mGlu_5Rs$ with anti-sense oligonucleotides resulted in reduced cell density in the IGL by about 50% and reduced the width of the molecular layer (Catania et al., 2001). However, it is difficult to compare our study with the previous one *in vivo* because we performed transient $mGlu_5R$ inhibition as opposed to a 50–80% elimination of $mGlu_5R$ expression in the cerebellum (based on the authors western blot data).

Finally, our results support a direct action of $mGlu_5R$ ligands on GCPs *in vivo* because we found $mGlu_5Rs$ expression in the EGL. However, we cannot exclude the possibility that $mGlu_5R$ manipulations *in vivo* indirectly regulate GCP survival through the release of a prosurvival molecule from other cells or their processes in proximity to GCPs. $mGlu_5Rs$ are expressed in cerebellar Golgi cells, but their expression in other cell types including Purkinje cells, which are known to release sonic hedgehog (Wechsler-Reya and Scott, 1999), remains unclear (Catania et al., 2001; Knopfel and Grandes, 2002).

CONCLUSION

We find that inhibition of $mGlu_5Rs$ in the postnatal cerebellum increases survival of GCPs while activation of $mGlu_5Rs$ increases the number of apoptotic cells in the EGL. These data provide unique insight into the consequences of administering MPEP during a developmentally sensitive time period. Given the potential use of $mGlu_5R$ antagonists for treatment of developmental disorders like Fragile X syndrome and autism (Dolen and Bear, 2008b), it is important for future studies to further elucidate the functional outcomes of systemic drug administration on neuron production.

Acknowledgments

This work was supported by grant from the NIH R01 NS062731 (A.B.) and F32 NS067986 (C.K.).

References

Altman J. Autoradiographic and histological studies of postnatal neurogenesis. 3. Dating the time of production and onset of differentiation of cerebellar microneurons in rats. J Comp Neurol. 1969; 136:269–293. [PubMed: 5788129]

Baillieux H, De Smet HJ, Paquier PF, De Deyn PP, Marien P. Cerebellar neurocognition: insights into the bottom of the brain. Clin Neurol Neurosurg. 2008; 110:763–773. [PubMed: 18602745]

Battaglia G, Bruno V, Pisani A, Centonze D, Catania MV, Calabresi P, Nicoletti F. Selective blockade of type-1 metabotropic glutamate receptors induces neuroprotection by enhancing gabaergic transmission. Mol Cell Neurosci. 2001; 17:1071–1083. [PubMed: 11414795]

Boer K, Troost D, Timmermans W, Gorter JA, Spliet WG, Nellist M, Jansen F, Aronica E. Cellular localization of metabotropic glutamate receptors in cortical tubers and subependymal giant cell tumors of tuberous sclerosis complex. Neuroscience. 2008; 156:203–215. [PubMed: 18706978]

Brazel CY, Nunez JL, Yang Z, Levison SW. Glutamate enhances survival and proliferation of neural progenitors derived from the subventricular zone. Neuroscience. 2005; 131:55–65. [PubMed: 15680691]

Bruno V, Ksiazek I, Battaglia G, Lukic S, Leonhardt T, Sauer D, Gasparini F, Kuhn R, Nicoletti F, Flor PJ. Selective blockade of metabotropic glutamate receptor subtype 5 is neuroprotective. Neuropharmacology. 2000; 39:2223–2230. [PubMed: 10974306]

Canudas AM, Giorgi-Gerevini V, Iacovelli L, Nano G, D'Onofrio M, Arcella A, Giangaspero F, Busceti C, Ricci-Vitiani L, Battaglia G, Nicoletti F, Melchiorri D. PHCCC, a specific enhancer of type 4 metabotropic glutamate receptors, reduces proliferation and promotes differentiation of cerebellar granule cell neuroprecursors. J Neurosci. 2004; 24:10343–10352. [PubMed: 15548648]

Carlson GC. Glutamate receptor dysfunction and drug targets across models of autism spectrum disorders. Pharmacol Biochem Behav. 2012; 100:850–854. [PubMed: 21315104]

Casanova MF. The neuropathology of autism. Brain Pathol. 2007; 17:422–433. [PubMed: 17919128]

Castiglione M, Calafiore M, Costa L, Sortino MA, Nicoletti F, Copani A. Group I metabotropic glutamate receptors control proliferation, survival and differentiation of cultured neural progenitor cells isolated from the subventricular zone of adult mice. Neuropharmacology. 2008; 55:560–567. [PubMed: 18603270]

Catania MV, Bellomo M, Di Giorgi-Gerevini V, Seminara G, Giuffrida R, Romeo R, De BA, Nicoletti F. Endogenous activation of group-I metabotropic glutamate receptors is required for differentiation and survival of cerebellar Purkinje cells. J Neurosci. 2001; 21:7664–7673. [PubMed: 11567056]

Copani A, Casabona G, Bruno V, Caruso A, Condorelli DF, Messina A, Di GG, Pin VJP, Kuhn R, Knopfel T, Nicoletti F. The metabotropic glutamate receptor mGlu5 controls the onset of developmental apoptosis in cultured cerebellar neurons. Eur J Neurosci. 1998; 10:2173–2184. [PubMed: 9753103]

Corti C, Aldegheri L, Somogyi P, Ferraguti F. Distribution and synaptic localisation of the metabotropic glutamate receptor 4 (mGluR4) in the rodent CNS. Neuroscience. 2002; 110:403–420. [PubMed: 11906782]

D'Antoni S, Berretta A, Seminara G, Longone P, Giuffrida-Stella AM, Battaglia G, Sortino MA, Nicoletti F, Catania MV. A prolonged pharmacological blockade of type-5 metabotropic glutamate receptors protects cultured spinal cord motor neurons against excitotoxic death. Neurobiol Dis. 2011; 42:252–264. [PubMed: 21232601]

Dave KA, Bordey A. GABA increases Ca^{2+} in cerebellar granule cell precursors via depolarization: implications for proliferation. IUBMB. 2009; 61:496–503.

Di Giorgi Gerevini V, Caruso A, Cappuccio I, Ricci Vitiani L, Romeo S, Della Rocca C, Gradini R, Melchiorri D, Nicoletti F. The mGlu5 metabotropic glutamate receptor is expressed in zones of active neurogenesis of the embryonic and postnatal brain. Brain Res Dev Brain Res. 2004; 150:17–22.

Di Giorgi-Gerevini V, Melchiorri D, Battaglia G, Ricci-Vitiani L, Ciceroni C, Busceti CL, Biagioni F, Iacovelli L, Canudas AM, Parati E, De Maria R, Nicoletti F. Endogenous activation of metabotropic glutamate receptors supports the proliferation and survival of neural progenitor cells. Cell Death Differ. 2005; 12:1124–1133. [PubMed: 15947794]

Dolen G, Bear MF. Role for metabotropic glutamate receptor 5 (mGluR5) in the pathogenesis of fragile X syndrome. J Physiol. 2008a; 586:1503–1508. [PubMed: 18202092]

Dolen G, Bear MF. Role for metabotropic glutamate receptor 5 (mGluR5) in the pathogenesis of fragile X syndrome. J Physiol. 2008b; 586:1503–1508. [PubMed: 18202092]

Elia J, Glessner JT, Wang K, Takahashi N, Shtir CJ, Hadley D, Sleiman PM, Zhang H, Kim CE, Robison R, Lyon GJ, Flory JH, Bradfield JP, Imielinski M, Hou C, Frackelton EC, Chiavacci RM, Sakurai T, Rabin C, Middleton FA, Thomas KA, Garris M, Mentch F, Freitag CM, Steinhausen HC, Todorov AA, Reif A, Rothenberger A, Franke B, Mick EO, Roeyers H, Buitelaar J, Lesch KP, Banaschewski T, Ebstein RP, Mulas F, Oades RD, Sergeant J, Sonuga-Barke E, Renner TJ, Romanos M, Romanos J, Warnke A, Walitza S, Meyer J, Palmason H, Seitz C, Loo SK, Smalley SL, Biederman J, Kent L, Asherson P, Anney RJ, Gaynor JW, Shaw P, Devoto M, White PS, Grant SF, Buxbaum JD, Rapoport JL, Williams NM, Nelson SF, Faraone SV, Hakonarson H. Genome-wide copy number variation study associates metabotropic glutamate receptor gene networks with attention deficit hyperactivity disorder. Nat Genet. 2012; 44:78–84. [PubMed: 22138692]

Fatemi SH, Reutiman TJ, Folsom TD, Sidwell RW. The role of cerebellar genes in pathology of autism and schizophrenia. Cerebellum. 2008; 7:279–294. [PubMed: 18418686]

Gandhi R, Luk KC, Rymar VV, Sadikot AF. Group I mGluR5 metabotropic glutamate receptors regulate proliferation of neuronal progenitors in specific forebrain developmental domains. J Neurochem. 2008; 104:155–172. [PubMed: 17944877]

Goldowitz D, Hamre K. The cells and molecules that make a cerebellum. Trends Neurosci. 1998; 21:375–382. [PubMed: 9735945]

Hatten ME, Heintz N. Mechanisms of neural patterning and specification in the developing cerebellum. Annu Rev Neurosci. 1995; 18:385–408. [PubMed: 7605067]

Huber KM. The fragile X-cerebellum connection. Trends Neurosci. 2006; 29:183–185. [PubMed: 16500716]

Kanumilli S, Roberts PJ. Mechanisms of glutamate receptor induced proliferation of astrocytes. Neuroreport. 2006; 17:1877–1881. [PubMed: 17179862]

Knopfel T, Grandes P. Metabotropic glutamate receptors in the cerebellum with a focus on their function in Purkinje cells. Cerebellum. 2002; 1:19–26. [PubMed: 12879970]

Koekkoek SK, Yamaguchi K, Milojkovic BA, Dortland BR, Ruigrok TJ, Maex R, De GW, Smit AE, VanderWerf F, Bakker CE, Willemsen R, Ikeda T, Kakizawa S, Onodera K, Nelson DL, Mientjes E, Joosten M, De SE, Oostra BA, Ito M, De Zeeuw CI. Deletion of FMR1 in Purkinje cells enhances parallel fiber LTD, enlarges spines, and attenuates cerebellar eyelid conditioning in Fragile X syndrome. Neuron. 2005; 47:339–352. [PubMed: 16055059]

Komuro H, Rakic P. Intracellular Ca^{2+} fluctuations modulate the rate of neuronal migration. Neuron. 1996; 17:275–285. [PubMed: 8780651]

Komuro H, Rakic P. Orchestration of neuronal migration by activity of ion channels, neurotransmitter receptors, and intracellular Ca2+ fluctuations. J Neurobiol. 1998; 37:110–130. [PubMed: 9777736]

Luyt K, Slade TP, Dorward JJ, Durant CF, Wu Y, Shigemoto R, Mundell SJ, Varadi A, Molnar E. Developing oligodendrocytes express functional GABA(B) receptors that stimulate cell proliferation and migration. J Neurochem. 2007; 100:822–840. [PubMed: 17144904]

Marti-Bonmati L, Menor F, Dosda R. Tuberous sclerosis: differences between cerebral and cerebellar cortical tubers in a pediatric population. AJNR Am J Neuroradiol. 2000; 21:557–560. [PubMed: 10730651]

Melchiorri D, Cappuccio I, Ciceroni C, Spinsanti P, Mosillo P, Sarichelou I, Sale P, Nicoletti F. Metabotropic glutamate receptors in stem/progenitor cells. Neuropharmacology. 2007; 53:473–480. [PubMed: 17675103]

Mullen RJ, Hamre KM, Goldowitz D. Cerebellar mutant mice and chimeras revisited. Perspect Dev Neurobiol. 1997; 5:43–55. [PubMed: 9509517]

Nguyen L, Rigo JM, Rocher V, Belachew S, Malgrange B, Rogister B, Leprince P, Moonen G. Neurotransmitters as early signals for central nervous system development. Cell Tissue Res. 2001; 305:187–202. [PubMed: 11545256]

Parkash J, Asotra K. Calcium wave signaling in cancer cells. Life Sci. 2010; 87:587–595. [PubMed: 20875431]

Platel JC, Dupuis A, Boisseau S, Villaz M, Albrieux M, Brocard J. Synchrony of spontaneous calcium activity in mouse neocortex before synaptogenesis. Eur J Neurosci. 2007; 25:920–928. [PubMed: 17331190]

Platel JC, Gordon V, Heintz T, Bordey A. GFAP-GFP neural progenitors are antigenically homogeneous and anchored in their enclosed mosaic niche. Glia. 2009; 57:66–78. [PubMed: 18661547]

Platel JC, Stamboulian S, Nguyen I, Bordey A. Neurotransmitter signaling in postnatal neurogenesis: The first leg. Brain Res Rev. 2010; 63:60–71. [PubMed: 20188124]

Platel J, Heintz T, Young S, Gordon V, Bordey A. Tonic activation of GLUK5 kainate receptors decreases neuroblast migration in a whole mount preparation of the subventricular zone. J Physiol (Lond). 2008; 586:3783–3793. [PubMed: 18565997]

Preibisch S, Saalfeld S, Tomancak P. Globally optimal stitching of tiled 3D microscopic image acquisitions. Bioinformatics. 2009; 25:1463–1465. [PubMed: 19346324]

Tanaka M, Marunouchi T. Immunohistochemical analysis of developmental stage of external granular layer neurons which undergo apoptosis in postnatal rat cerebellum. Neurosci Lett. 1998; 242:85–88. [PubMed: 9533400]

Wechsler-Reya RJ, Scott MP. Control of neuronal precursor proliferation in the cerebellum by Sonic Hedgehog. Neuron. 1999; 22:103–114. [PubMed: 10027293]

Wood KA, Dipasquale B, Youle RJ. In situ labeling of granule cells for apoptosis-associated DNA fragmentation reveals different mechanisms of cell loss in developing cerebellum. Neuron. 1993; 11:621–632. [PubMed: 8398151]

Zhao L, Jiao Q, Yang P, Chen X, Zhang J, Zhao B, Zheng P, Liu Y. Metabotropic glutamate receptor 5 promotes proliferation of human neural stem/progenitor cells with activation of mitogen-activated protein kinases signaling pathway in vitro. Neuroscience. 2011

Highlights

1. Functional expression of $mGlu_5R$ in the neonatal cerebellar neurogenic zone
2. $mGlu_5R$ inhibition enhances the survival of granule cell precursors (GCP)
3. Gene array analysis supports $mGlu_5R$ function on GCP apoptosis

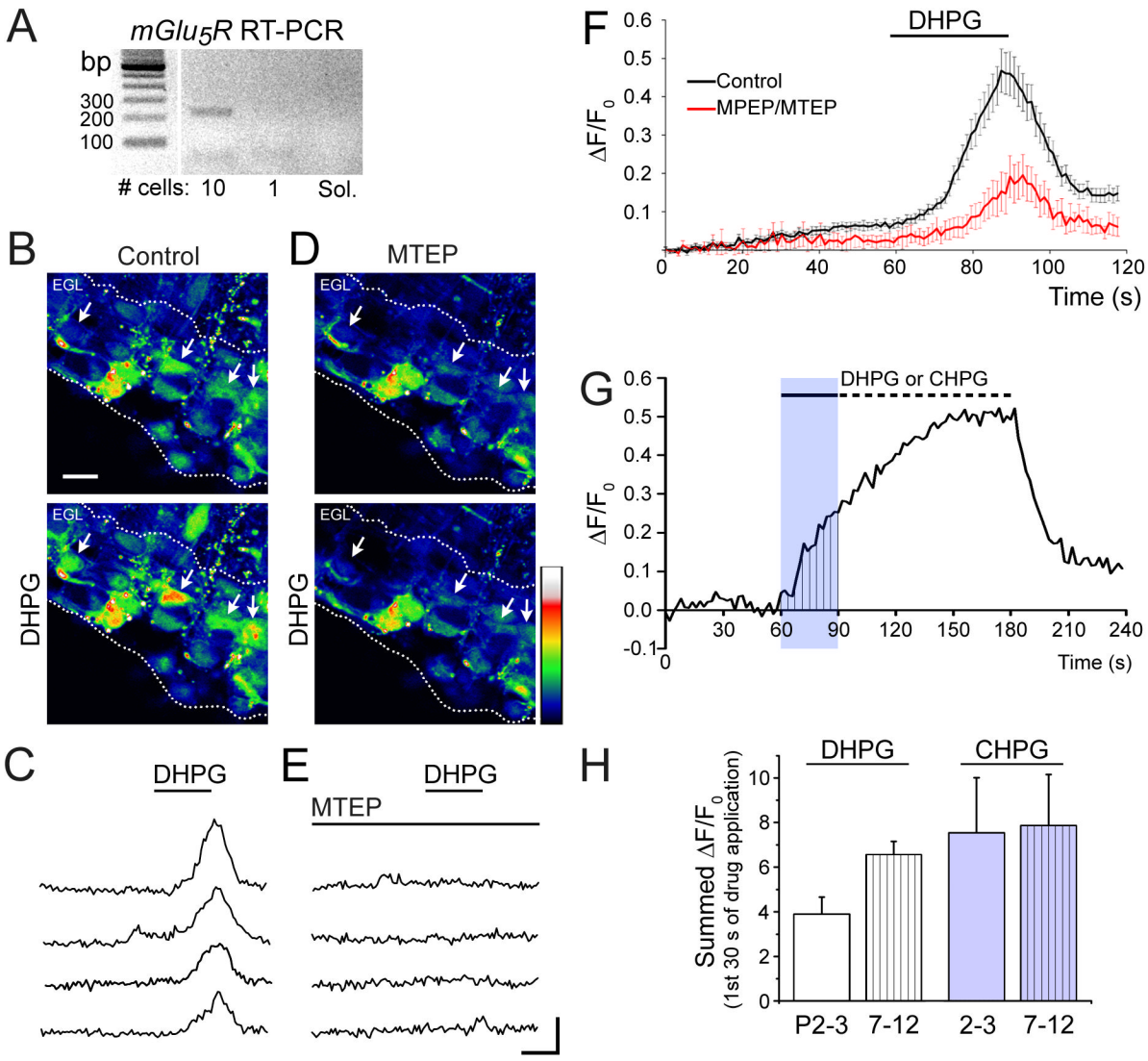

Figure 1. Functional mGlu$_5$Rs are expressed in the postnatal EGL

(A)DNA gels of RT-PCR for *mGlu$_5$R* (216 bp) from 10 cell-aspirates and 1 cell-aspirate or solution (sol.) only.**(B and D)** Pseudocolored images of Fluo 4/OGB-loaded GCPs before (top) and after (bottom) DHPG application (30 s, 100 μM) in control (B) and in the presence of 60 μM MTEP (D). Arrows indicate several cells that have DHPG-induced Ca^{2+} increase in control solution. The EGL is demarcated by white dotted lines. Scale bar = 10 μm. Intensity color scale bar: 0 to 255 (saturation). **(C and E)** Ca^{2+} activity traces for cells indicated with arrows in (B and D). Scale bar: 20 s/0.2 $\Delta F/F_0$ with F, fluorescence and F_0, baseline fluorescence. **(F)** Mean (± sem) Ca^{2+} activity graphs illustrating DHPG responses in the absence and presence of MTEP or MPEP. n= 6 slices. **(G)** Diagram illustrating the analyzed area under the curve during the first 30 s of agonist application. **(H)** Bar graphs of the area under the Ca^{2+} responses for DHPG and CHPG at both age groups, P2–P3 and P7–P12.

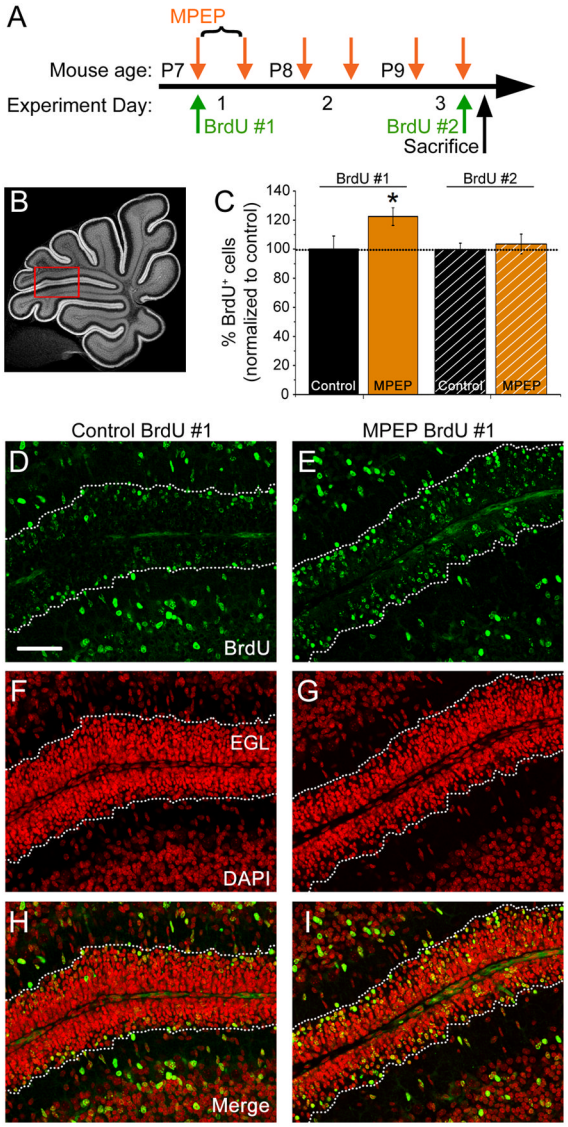

Figure 2. mGlu$_5$R inhibition *in vivo* increases the number of proliferative cells in the EGL

(A) Experimental plan for intraperitoneal (IP) injection of BrdU and MPEP in P7–P9 mice. **(B)** Mid-sagittal cerebellar section labeled with DAPI indicating the region of quantification between folia V-VI (red box). **(C)** Bar graphs of the percentage (%) of BrdU-positive cells in the EGL normalized to control following control PBS or MPEP injections. BrdU was injected prior to the first or following the last MPEP injection. *$p < 0.05$. **(D–I)** Confocal micrographs of BrdU immunostaining (green, D–E), DAPI counterstaining (red. F–G) and merge (H–I) between folia V–VI from control or MPEP-treated mice. The EGL is outlined with white dotted lines. Scale bar = 50 μm.

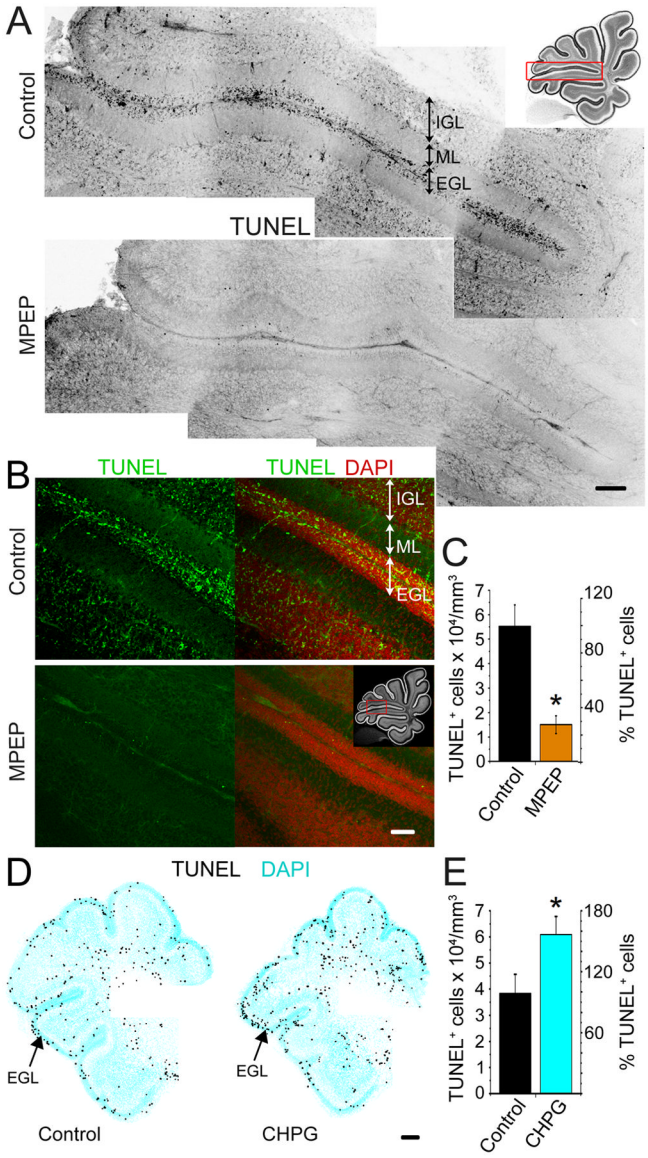

Figure 3. mGlu$_5$R inhibition promotes GCL survival in the EGL

(A) Montage of TUNEL staining (black) along the entire folia V–VI interface in control (top) and MPEP-treated (bottom) conditions. Inset shows imaged area. Scale bar: 100 μm. **(B)** Confocal micrographs of TUNEL (green) and DAPI (red) staining in the area between folia V–VI in control (top) and MPEP-treated (bottom) sagittal sections. Inset shows imaged area. Scale bar: 50 μm. **(C)** Average number of TUNEL$^+$ cells per mm^3 and % TUNEL$^+$ cells in the EGL of control (black) and MPEP-treated animals (orange). **(D)** Reconstructions of transversal cerebellar sections stained for TUNEL (black) and DAPI (cyan) from P3 control or CHPG-treated mice. Scale bar: 100 μm. **(E)** Average number of TUNEL$^+$ cells per mm^3 and % TUNEL$^+$ cells in the EGL of control (control) and CHPG-treated animals (cyan). *$p < 0.05$.

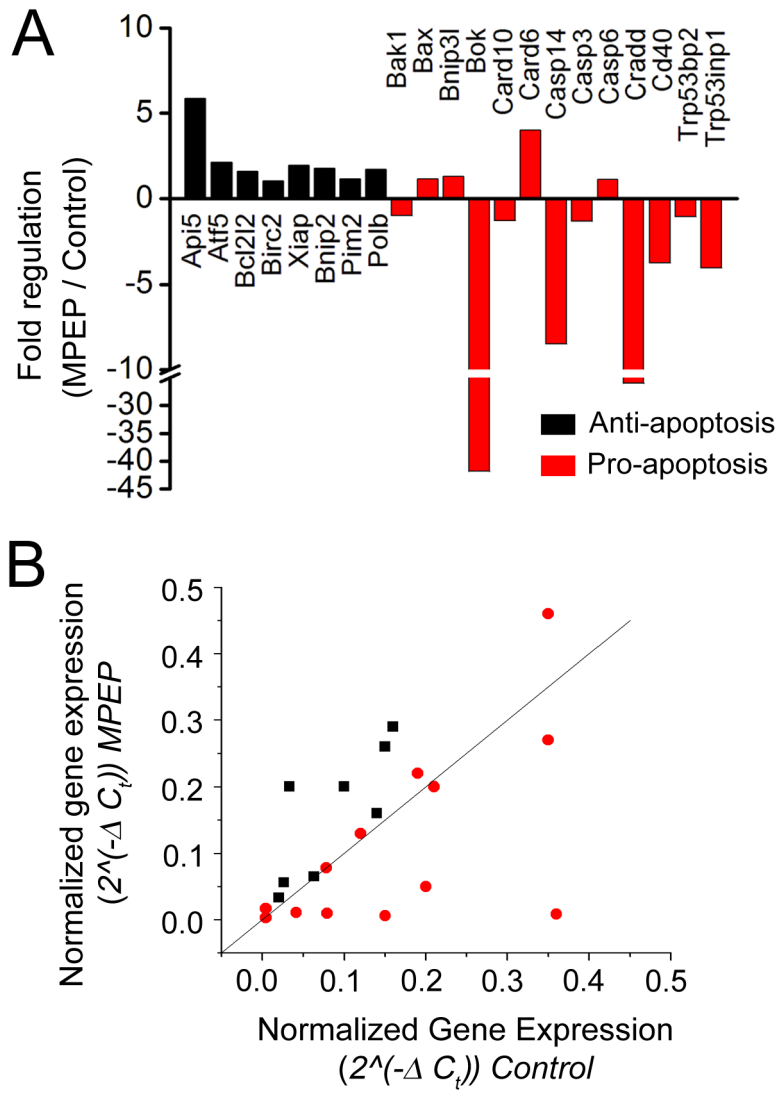

Figure 4. Effects of *in vivo* MPEP treatment on apoptosis-related gene expression

(A) Fold changes in 21 anti-apoptosis (black) or pro-apoptosis (red) genes in MPEP-treated samples normalized to control. **(B)** Plot of normalized gene expression in MPEP-treated samples versus normalized gene expression in control samples for the 21 genes in (A).

Table 1

Apoptosis-related genes examined.

Symbol	RefSeq	Description	Role in apoptosis	Fold regulation (MPEP/CONTROL)	p value
Api5	NM_007466	Apoptosis inhibitor 5	anti	5.86	0.159
Atf5	NM_030693	Activating transcription factor 5	anti	2.11	0.239
Bcl2l2	NM_007537	Bcl2-like 2	anti	1.61	0.223
Birc2	NM_007465	Baculoviral IAP repeat-containing 2	anti	1.02	0.349
Xiap	NM_009688	X-linked inhibitor of apoptosis	anti	1.96	0.383
Bnip2	NM_016787	BCL2/adenovirus E1B interacting protein 2	anti	1.76	0.138
Pim2	NM_138606	Proviral integration site 2	anti	1.16	0.165
Polb	NM_011130	Polymerase (DNA directed), beta	anti	1.71	0.298
Bak1	NM_007523	BCL2-antagonist/killer 1	pro	−1.00	0.288
Bax	NM_007527	Bcl2-associated X protein	pro	1.15	0.266
Bnip3l	NM_009761	BCL2/adenovirus E1B interacting protein 3-like	pro	1.30	0.273
Bok	NM_016778	BCL2-related ovarian killer protein	pro	−41.79	0.024
Card10	NM_130859	Caspase recruitment domain family, member 10	pro	−1.30	0.388
Card6	XM_139295	Caspase recruitment domain family, member 6	pro	4.01	0.212
Casp14	NM_009809	Caspase 14	pro	−8.49	0.049
Casp3	NM_009810	Caspase 3	pro	−1.32	0.372
Casp6	NM_009811	Caspase 6	pro	1.11	0.399
Cradd	NM_009950	CASP2 and RIPK1 domain containing adaptor with death domain	pro	−25.99	0.063
Cd40	NM_011611	CD40 antigen	pro	−3.76	0.167
Trp53bp2	NM_173378	Transformation related protein 53 binding protein 2	pro	−1.07	0.314
Trp53inp1	NM_021897	Transformation related protein 53 inducible nuclear protein 1	pro	−4.06	0.187
Gusb	NM_010368	Glucuronidase, beta	hk*	1.06	0.336
Hprt1	NM_013556	Hypoxanthine guanine phosphoribosyl transferase 1	hk*	1.06	0.355
Gapdh	NM_008084	Glyceraldehyde-3-phosphate dehydrogenase	hk*	−1.12	0.158
Actb	NM_007393	Actin, beta	hk*	2.05	0.114

*housekeeping gene